





In Silico and in Vitro Evaluation of Selected Herbal Compounds as Robust HER-2 Inhibitors for Effective Treatment of Breast Cancer

Mona Pourjafar¹ , Naghmeh Shirafkan², Somaye Bakhtiari³, Saeid Afshar¹, Massoud Saidijam¹, Alireza Jalalvand⁴, Amir Taherkhani^{1*} 

¹Research Center for Molecular Medicine, Hamadan University of Medical Sciences, Hamadan, Iran.

²Department of Immunology, School of Medicine, Hamadan University of Medical Sciences, Hamadan, Iran.

³Vice-Chancellor for Research & Technology, Hamadan University of Medical Sciences, Hamadan, Iran.

⁴Department of Influenza and Other Respiratory Viruses, Pasteur Institute of Iran, Tehran, Iran.

Abstract

Background and objectives: Breast cancer is the most frequently reported malignancy in women worldwide and is a heterogeneous disease. Due to different levels of human epidermal growth factor receptor 2 (HER-2) and its critical role in tumor progression, HER-2 has been considered as a validated target in breast cancer therapy. The present study aimed to identify new and effective HER-2 inhibitors from selected plant-based compounds using a computational drug discovery approach. The anticancer effects of top-ranked compounds were then evaluated using cellular and molecular methods. **Methods:** The binding affinities of 47 herbal compounds (including 21 flavonoids, 16 anthraquinones, and 10 cinnamic acids) with the extracellular domain of HER-2 were evaluated using molecular docking analysis. The top hits were evaluated for their cell proliferation inhibition, apoptosis, and migration effects in high and low HER-2-overexpressing SKBR-3 and MCF-7 cell lines, respectively. **Results:** Chrysin, chrysophanol, and chlorogenic acid revealed the highest binding affinity to the extracellular domain of HER-2; therefore, they were considered the top-ranked HER-2 inhibitors in this study. Each component inhibited cell proliferation and decreased migration activity of SKBR-3 and MCF-7 cell lines, while the SKBR-3 cells were affected more. The results of the apoptosis assay showed that chrysin was the only compound that could cause a significant induction of SKBR-3 cell apoptosis in comparison to MCF-7 cells. **Conclusion:** The results of the present study suggest that chrysophanol, chlorogenic acid, and especially chrysin may have anticancer effects and could be considered drug candidates for therapeutic aims in human HER-2 positive cancer.

Keywords: breast cancer; epidermal growth factor receptor 2; molecular docking

Citation: Pourjafar M, Shirafkan N, Bakhtiari S, Afshar S, Saidijam M, Jalalvand A, Taherkhani A. In silico and in vitro evaluation of selected herbal compounds as robust HER-2 inhibitors for effective treatment of breast cancer. Res J Pharmacogn. 2023; 10(3): 43–59.

Introduction

Breast cancer is the most frequent malignancy in women globally. According to the World Health Organization, breast cancer became the most common cancer in 2021, accounting for 12% of all new annual cancer cases worldwide. Besides, more than 2.2 million new cases and 684,996

recent deaths were reported in 2020 [1,2]. Clinically, specific subtypes of breast cancer are defined by their histopathological appearance and expression of molecular targets. The first molecular target is hormone receptors (estrogen receptor alpha (ER α) and progesterone receptor

*Corresponding author: a.taherkhani@umsha.ac.ir

(PR)), which are expressed in approximately 70% of invasive breast cancers. The second main molecular target is epidermal growth factor 2 (ERBB2, formerly HER-2 or HER-2 /neu), a transmembrane tyrosine kinase receptor in the epidermal growth factor receptor family. Its expression is detected in approximately 20% of breast cancers. Concerning the presence or absence of these receptors, breast cancers are classified as luminal A (HER-2 negative, and ER and/or PR positive) luminal B (HER-2 positive, and ER and/or PR positive); HER-2 -enriched (HER-2 positive, and ER and PR negative) and basal like (triple-negative breast cancer- HER-2, ER, and PR negative) [3-5].

HER-2-positive breast cancer, compared with HER-2-negative tumors, is an aggressive subtype with a poor response to standard chemotherapy regimens [6]. HER-2 is always in an active conformation and ready to interact with the ligand-activated HER receptors; highly expressed HER-2 at the cell membrane results in constitutive signaling of downstream pathways. Differential levels of HER-2 and its role in tumor progression make HER-2 a validated target in breast cancer therapy. A better understanding of intracellular and extracellular studies on the HER-2 gene and its signaling has provided insights into strategies to inhibit this pathway and has developed new HER-2-targeted pharmacological agents. This could subsequently result in better survival outcomes in patients with advanced HER-2-positive breast cancer [7,8].

To design and develop novel potential HER-2 inhibitors, in silico methods are considered as one of the least expensive and fastest ways in the therapy field. Various drugs derived from natural products are being used in treatments successfully [9,10]. Traditional herbal compounds demonstrate anti-inflammatory, antioxidant, and anticancer properties that could be used as cancer therapeutic agents [11]. Flavonoids with the basic structure of (C₆-C₃-C₆) skeleton are the most significant subgroup of polyphenolics in the plant kingdom [12,13]. Anthraquinones are plant-based metabolites mainly found in *Rubiaceae*, *Polygonaceae*, and *Rhamnaceae* families. They all contain a primary structure of 9,10-anthracenedione, leading to several derivatives with various therapeutic applications [14].

Moreover, cinnamic acid derivatives with an elementary construction of C₆-C₃

(phenylpropanoid) are essentially identified in *Cinnamomum cassia*, *Panax ginseng*, and honey [15,16]. Several beneficial effects of flavonoids, anthraquinones, and cinnamic acid have made them potential drug candidates for cancer therapy. In the present study, we hypothesized that the binding of small molecules to the central residues incorporated in the extracellular domain of HER-2 might attenuate the receptor dimerization and downstream signaling pathway. To examine this hypothesis, we selected a list of natural compounds from medicinal herbs with anticancer activities in previous studies, including flavonoids [17], anthraquinones [18], and cinnamic acid derivatives [19,20]. We performed a comparative docking study using an in silico approach for the virtual screening of selected herbal compounds [21] to establish the best molecular interactions between the HER-2 inhibitors and the HER-2 receptor. Moreover, the selected inhibitors were applied on SKBR-3 cell lines, which overexpress HER-2, and MCF-7 cell lines, which lack HER-2, to assess the impact on cell proliferation and migration, and investigate the genes implicated in these pathways.

Material and Methods

Ethical considerations

Ethics were considered in this study. The present study was approved by the Ethics Committee of Hamadan University of Medical Sciences, Hamadan, Iran, on 2021.01.25 (IR.UMSHA.REC.1398.958).

Chemicals

Tetrazolium 3-(4, 5-dimethylthiazol-2-yl)-2, 5-diphenyltetrazolium bromide (MTT) assay kit (Sigma, USA); Annexin-V-FITC/Propidium Iodide (PI) kit (MabTag, Germany); RNX-Plus Kit (Cinnagen, Tehran, Iran); First-strand cDNA synthesis kit (Cinnagen, Tehran, Iran); SYBR green master mix (Ampliqon, Denmark); DMEM (Bioidea, Iran); DMSO (Sigma Aldrich, USA); Chrysin (Sigma-Aldrich; Merck; CAS. no. 480400); Chrysophanol (Sigma-Aldrich; Merck; CAS. no. 481743); Chlorogenic acid (Sigma-Aldrich; Merck; CAS. no. 327979) were used in the study.

Computational procedures

To evaluate our hypothesis, we selected the crystalline structure of HER-2 complexed with pertuzumab (PDB ID: 1S78). Pertuzumab is an anti-HER-2 monoclonal antibody, which binds to

HER-2 close to the center of domain II, sterically blocking a binding pocket essential for receptor dimerization and downstream signaling pathway [22]. The research collaboratory achieved the three-dimensional (3D) structure of the HER-2 extracellular domain for Structural Bioinformatics (<https://www.rcsb.org>) [23]. The PDB code 1S78 with criteria of x-ray resolution as 3.25 Å was selected to study the binding affinity of 47 natural components with the extracellular domain of HER-2. In addition, molecular docking analysis was executed between HER-2 and HERP5 as a positive control compound. According to the results of the study by Satyanarayanajois et al. HERP5 demonstrated a considerable binding affinity to the HER-2 extracellular domain. Moreover, HERP5 showed anti-proliferative activity with the IC₅₀ value of 0.396 micromolar against SKBR-3 cell lines [24]. The 1S78 file contained six polypeptide chains: A, B, C, D, E, and F. The chains A and B represented the extracellular domain of HER-2, where C, D, E, and F served as pertuzumab Fab light chains. Chain B, with a length of 624 residues, was considered for molecular docking analysis, and the other chains were removed from the PDB file before molecular docking analysis. Energy minimizing (EM) of the protein was executed before docking procedures utilizing the Swiss-pdbViewer version 4.1.0 (<https://spdbv.unil.ch/>) [25]. Before the docking process, the PDBQT files of the receptor and ligands were prepared [26].

The 3D coordinates of small molecules were primarily obtained from the PubChem database (<https://pubchem.ncbi.nlm.nih.gov>) as structure data file (SDF) files. Next, the PDB formats of the structures were achieved using the cactus webserver (<http://cactus.nci.nih.gov/translate/>). Moreover, the EM was applied for all ligands with MM+ force field by the HyperChem 8.0.10 software [27].

A windows-based operating system with the criteria of system type, 64-bit; processor, Intel Core i7; installed memory, 32 GB was utilized for the docking study, which was performed using the AutoDock 4.0 (<http://autodock.scripps.edu>) [28]. Within the HER-2 extracellular domain, the interacting residues with the pertuzumab Fab light chain (which are necessary for receptor dimerization and signaling) were considered as a receptor site in docking analyses; these key amino acids were identified from the study by Franklin et al. [22]

and included His245, Tyr252, Phe257, Thr268, Asp285, Val286, Ser288, Thr290, Pro294, Leu295, His296, Lys314, and Pro315. The grid box in the AutoDock tool was set to X-dimension, 60; Y-dimension, 74; Z-dimension, 86; X-center, 14.144; Y-center, 21.709; Z-center, 209.157; spacing, 0.375 Å. The number of docked runs for each ligand was set to 50. The model with the lowest binding energy in the main cluster of the RMSD table was considered for further analyses, including protein-ligand complex imaging and interaction mode analysis. The BIOVIA Discovery Studio Visualizer version 19.1.0.18287

(<https://discover.3ds.com/discovery-studio-visualizer-download>) was used for analyzing the interactions among ligands and residues of HER-2 extracellular domain to achieve the 2D/3D view of the docked poses.

Experimental procedures

Cell viability assay

This study assessed the selected inhibitors cytotoxicity using tetrazolium 3-(4, 5-dimethylthiazol-2-yl)-2, 5-diphenyltetrazolium bromide (MTT) assay kit [29]. Briefly, 1×10^4 SKBR-3 (Iranian Biological Resource Center) (high expressed HER-2) and MCF-7 (Iranian Biological Resource Center) (low expressed HER-2) cells were seeded in 96-well tissue culture plates per well and cultured overnight. Different concentrations of selected HER-2 inhibitors were prepared using a 10% FBS-high glucose DMEM medium and added to the cells. After cell incubation for 24, 48, and 72 h at 37 °C, 10 µL of MTT dye was added to each well (0.9 mg/mL), followed by 3 hours of incubation at 37 °C. The viable cells with active metabolism converted MTT into a purple-colored formazan product. The medium was discarded, and the insoluble formazan precipitate was then solubilized with Dimethyl sulfoxide DMSO. An ELISA microplate reader (Biotek, USA) measured the absorbance at 570 nm with a reference wavelength of 630 nm. The cell viability percentage was calculated as follows.

$$\text{Cell viability (\%)} = \frac{\text{absorbance of treated cells}}{\text{absorbance of untreated cells}} \times 100$$

Wound healing assay

The scratch-wound assay measured SKBR-3 and MCF-7 cell migration. In this method, 70×10^3

SKBR-3 and MCF-7 cells were seeded in a 24-well plate separately and incubated at 37 °C for 24 h. On the following day, the confluent monolayer cells were scratched with a sterile pipette crystal tip to make a thin incision, and then it was washed with PBS to remove the debris. Afterward, each well was treated with selected HER-2 inhibitors. Cells on the plate were photographed randomly from various areas with inverted microscope (time 0) and then incubated for 24, 48, and 72 h at 37°C with 5% CO₂, allowing them to migrate into the wound area. Images of the wound were collected at these three-time points with inverted microscope (Motic, China). Cell migration was determined through the wound edge polarization and migration into the wound space [30].

Cell apoptosis assay

Cell apoptosis was analyzed according to the manufacturer's instructions using an Annexin-V-FITC/Propidium Iodide (PI) kit. Briefly, SKBR-3 and MCF-7 cell lines were seeded in 6-well plates at a density of 3×10^5 . After treatment with selected HER-2 inhibitors (based on MTT results), cells were trypsinized and centrifuged at 300 g for 5 min at 4 °C. The cell pellet was resuspended in a cold binding buffer and stained with Annexin V-FITC and PI solutions. After 15 min of incubation, apoptosis and cell death were detected using Attune NxT acoustic focusing cytometer (Life Technology, USA), and data were analyzed using FlowJo software version 10 for Windows [30].

RNA isolation and quantitative reverse-transcription polymerase chain reaction (RT-qPCR)

Total RNA was isolated from the SKBR-3 and MCF-7 cell lines treated with chrysin using RNX-Plus Kit after 24 h. Quantity and quality of the isolated RNA were measured using NanoDrop and 2 µg of total RNAs was converted to complementary DNA (cDNA) with reverse transcriptase using a first-strand cDNA synthesis kit. The real-time PCR assay was conducted with SYBR green master mix and specific primers for CXCR4, MMP9, VEGF, and Caspase-3 with thermal cycling as follows; initial denaturation at 95 °C for 15 min, followed by 40 amplification cycles of denaturation at 95 °C for 30 s, annealing at 60 °C for 30 s and extension 72 °C for 30 s using a light cycler instrument (Roche 96 system, Germany). Primer sequences are listed in

Table 1. The expression level of the genes was normalized with β-actin as an internal control, and the relative expression of genes was reported using the $2^{-\Delta\Delta CT}$ method analysis.

Results and Discussion

The smaller $\Delta G_{\text{binding}}$, demonstrates the higher binding affinity between ligands and receptors. In this regard, $\Delta G_{\text{binding}} < -5.00$ kcal/mol illustrates a good binding power, while $\Delta G_{\text{binding}} < -7.00$ demonstrates a salient binding affinity [31]. According to the in silico analyses, 18 flavonoids, 10 anthraquinones, and 4 cinnamic acid derivatives exhibited a salient binding strength with the HER-2 extracellular domain. In addition, chrysin, chrysophanol, and chlorogenic acid exhibited the most significant results among flavonoids, anthraquinones, and cinnamic acid derivatives, respectively. Furthermore, the results showed that these three compounds had a greater binding affinity to HER-2 extracellular domain than HERP5 (Table 2). The $\Delta G_{\text{binding}}$ value between chrysin, chrysophanol, chlorogenic acid, HERP5, and the extracellular region of HER-2 was estimated as -8.12, -9.07, -10.20, and -7.36 kcal/mol, respectively. Table 3 details these top-ranked compounds' energies and inhibition constant (K_i) values.

All hydrogen and hydrophobic interactions among top-ranked components in this study, control inhibitor, and the main residues incorporated in the HER-2 extracellular domain were analyzed and demonstrated in Figure 1. In this regard, chrysin, chrysophanol, and chlorogenic acid formed five, three, and six hydrogen bonds with the extracellular residues of HER-2, respectively. The compounds' 3D views of docked poses are also presented in Figure 1. The details of classical and non-classical hydrogen bonds between ligands and the residues within the HER-2 extracellular domain are shown in Table 4. The IUPAC describes a hydrogen bond (H bond) as an attractive interaction in which hydrogen is covalently bound to an electronegative atom (H bond donor) and interacts with another electronegative atom (H bond acceptor). In classical (conventional) H bonds, the donor and acceptor are the most electronegative elements, including O, N, and F. In non-classical (nonconventional) H bonds, alternative atoms act as H bond acceptors with the same characteristics as conventional H bonds [32].

Table 1. Specific primer sequences for qRT-PCR

Gene	Sense strand	Antisense strand
CXCR4	CATGGAAATATACACTTCGGA	TGCCCACTATGCCAGTCAAG
MMP9	GGTGATTGACGACGCCTTTG	AACCGAGTTGGAACCACGA
VEGF	GTG CTA ATG TTA TTG GTG TCT TC	CTC TCA TCT CCT CCT CTT CC
Caspase-3	GAATGTCATCTCGCTCTGGTACG	CTGCTCCTTTTGCTATGATCTTCC

qRT-PCR: quantitative reverse transcription PCR

Table 2. Binding affinity between 47 herbal ligands and the positive control inhibitor with the extracellular domain of HER-2

A, Flavonoids					
PubChem ID	Ligand name	Estimated binding energy (kcal/mol)	Ki (uM)	Herbal source (s)	Reference
5281607	Chrysin	-8.12	1.13	Mushrooms	[33]
629440	Hemileiocarpin	-8.09	1.17	<i>Glycyrrhiza glabra</i>	[34]
5280443	Apigenin	-8.05	1.26	Parsley	[35]
5281612	Diosmetin	-8.03	1.29	<i>Citrus</i> fruits	[36]
9911508	Astragalin	-7.96	1.45	<i>Moringa oleifera</i> and <i>Cassia alata</i>	[37]
5317435	Fustin	-7.85	1.75	<i>Rhus verniciflua</i>	[38]
9064	Catechin	-7.81	1.88	<i>Mimosa catechu</i>	[39]
14309735	Xanthogalenol	-7.74	2.12	<i>Humulus lupulus</i>	[40]
638278	Isoliquiritigenin	-7.65	2.47	<i>Glycyrrhiza uralensis</i>	[41]
5281654	Isorhamnetin	-7.59	2.72	<i>Anoectochilus roxburghii</i>	[42]
1203	Epicatechin	-7.54	3.00	<i>Litchi chinensis</i> .	[43]
72936	Sophoraflavanone G	-7.53	3.01	<i>Sophora flavescens</i>	[44]
10680	Flavone	-7.20	5.27	<i>Scutellaria baicalensis</i>	[45]
5280681	3-O-Methylquercetin	-7.18	5.42	<i>Viscum coloratum</i> , <i>Sarcocornia fruticosa</i> , <i>Nasturium officinale</i> <i>Achyrocline</i> <i>satureioides</i> , <i>Semecarpus anacardium</i>	[46]
25201019	Ponciretin	-7.17	5.54	<i>Citrus</i> fruits	[47]
124052	Glabridin	-7.12	6.00	<i>Glycyrrhiza glabra</i>	[48]
72281	Hesperetin	-7.11	6.12	<i>Citrus</i> fruits	[49]
443639	Epiatzelechin	-7.03	6.99	<i>Bergenia ligulata</i>	[50]
5318998	Licochalcone A	-6.88	8.98	<i>Glycyrrhiza inflata</i>	[51]
639665	Xanthohumol	-6.60	14.59	<i>Humulus lupulus</i>	[52]
5280378	Formononetin	-6.51	17.03	Red propolis	[53]
B, Anthraquinones					
PubChem ID	Ligand name	Estimated binding energy (kcal/mol)	Ki (uM)	Herbal source (s)	Reference
10208	Chrysophanol	-9.07	0.11416	<i>Rumex</i> and <i>Rheum</i>	[54]
6293	Alizarin	-8.96	0.27058	<i>Radix Rubiae</i>	[55]
99649	Emodin-8-glucoside	-8.93	0.28690	<i>Moringa oleifera</i>	[56]
10168	Rhein	-8.31	0.80391	<i>Rheum palmatum</i> , <i>Cassia tora</i> , <i>Polygonum multiflorum</i> , <i>Aloe barbadensis</i>	[57]
361510	Emodic acid	-7.83	1.82	<i>Nephromopsis cucullata</i>	[58]
3220	Emodin	-7.81	1.89	<i>Rheum palmatum</i> , <i>Polygonum cuspidatum</i> , <i>Polygonum multiflorum</i>	[59]
101286218	Rhodoptilometrin	-7.75	2.10	<i>Himerometra magnipinna</i>	[60]
10639	Physcion	-7.31	4.38	<i>Radix et Rhizoma rhei</i>	[61]
10459879	Sennidin B	-7.24	4.94	Human intestinal anaerobe, <i>Bifidobacterium</i> sp. strain SEN	[62]
2950	Danthron	-7.12	6.04	<i>Rheum palmatum</i>	[63]
124062	Rubiadin	-6.81	10.20	Rubiaceae family	[64]
3083575	Obtusifolin	-6.52	16.56	<i>Cassia tora</i>	[65]
92826	Sennidin A	-5.4	109.95	<i>Senna angustifolia</i>	[66]
2948	Damnacanthal	-5.26	139.71	<i>Morinda citrifolia</i>	[67]
442753	Knipholone	-5.11	179.62	<i>Kniphofia foliosa</i>	[68]
160712	Nordamnacanthal	-4	1170	<i>Morinda elliptica</i>	[69]

Table 2. Continued

C, Cinnamic acid derivatives					
PubChem ID	Ligand name	Estimated binding energy (kcal/mol)	Ki (uM)	Herbal source (s)	Reference
1794427	Chlorogenic acid	-10.2	0.0333	<i>Malus domestica</i> , <i>Cynara</i> , <i>Piper betle</i> , <i>Arctium lappa</i> , <i>Daucus carota</i> , <i>Robusta coffee</i> , <i>Solanum melongena</i> , <i>Eucommia ulmoides</i> , <i>Vitis vinifera</i>	[70]
5281787	Caffeic acid phenethyl ester	-7.58	2.76	Propolis and grains	[71,72]
637540	o-Coumaric acid	-7.27	4.70	<i>Hordeum vulgare</i> , <i>Secale cereal</i> , <i>Zea mays</i> , <i>Vaccinium corymbosum</i> , <i>Malus domestica</i> , <i>Vitis vinifera</i> , <i>Phaseolus vulgaris</i> , <i>Pisum sativum</i> , <i>Solanum lycopersicum</i> , <i>Allium sativum</i> , <i>Camellia sinensis</i>	[73-76]
5281759	Caffeic acid 3-glucoside	-7.1	6.27	<i>Vaccinium macrocarpon</i>	[77]
5372945	N-p-Coumaroyltyramine	-6.63	13.71	<i>Crinum biflorum</i>	[78]
689043	Caffeic acid	-5.79	57.09	<i>Vaccinium corymbosum</i> , <i>Actinidia deliciosa</i> , <i>Prunus domestica</i> , <i>Prunus avium</i> , <i>Malus domestica</i>	[79]
444539	Cinnamic acid	-5.47	97.04	<i>Cinnamomum cassia</i> , <i>Panax ginseng</i> , grains, and honey	[80]
445858	Ferulic acid	-5.4	110.72	<i>Triticum spp</i> , <i>Zea mays</i> , <i>Spinacia oleracea</i> , <i>Vitis, vinifera</i> , <i>Rheum rhabarbarum</i> , <i>Avena sativa</i> , <i>Hordeum vulgare</i> , <i>Secale cereale</i> , <i>Zea mays</i> , <i>Oryza sativa</i>	[81]
637542	p-Coumaric acid	-5.38	114.04	<i>Hordeum vulgare</i> , <i>Secale cereal</i> , <i>Zea mays</i> , <i>Vaccinium corymbosum</i> , <i>Vitis vinifera</i> , <i>Malus domestica</i> , <i>Phaseolus vulgaris</i> , <i>Pisum sativum</i> , <i>Corylus avellana</i> , <i>Carya illinoensis</i> , <i>Apium graveolens</i> , <i>Solanum lycopersicum</i> , <i>Allium sativum</i> , <i>Linum usitatissimum</i> , <i>Camellia sinensis</i>	[73-76]
637775	Sinapinic acid	-5.02	208.48	Rhizome of <i>Hydnophytum formicarum</i>	[82]
NA	HERP5 (Ctrl+)	-7.36	4.01	NA	

Ctrl+: positive-control; NA, not available

Table 3. Details of energies and inhibition constant values between top-ranked compounds in this study, control positive inhibitor, and the extracellular domain of HER-2

Ligand name	Intermolecular energy (kcal/mol)	Internal energy (kcal/mol)	Torsional free energy (kcal/mol)	Unbound system's energy (kcal/mol)	Free binding energy (kcal/mol)	Ki (uM)
Chrysin	-8.02	-1.72	1.19	-0.43	-8.12	1.13
Chrysophanol	-9.04	-1.27	1.19	-0.05	-9.07	0.22522
Chlorogenic acid	-9.07	-6.44	4.18	-1.14	-10.2	0.033.3
HERP5 (Ctrl+)	-9.74	-1.48	2.98	-0.88	-7.36	4.01

Ctrl+: positive-control

Table 4. Interaction modes between the best inhibitors in this study and the extracellular domain of HER-2

Ligand name	Hydrogen bond (distance Å)	Hydrophobic interaction (distance Å)
Chrysin	Cys246 (4.57, Classical); Pro247 (4.38, Classical); Tyr267 (4.65, Non-Classical); Gly287 (3.13, Non-Classical; 3.67, Non-Classical)	Ala248 (4.18, Alkyl); Leu249 (4.25, Alkyl); Val250 (5.95, Alkyl)
Chrysophanol	Asn297 (3.71, Classical); Ala317 (3.87, Classical); Cys293 (4.41, Non-Classical)	Leu295 (4.22, Alkyl); Ala317 (3.83, Alkyl); Val319 (5.07, Alkyl); Cys316 (4.73, Alkyl)
Chlorogenic acid	Val286 (3.33, Classical; 4.60, Classical; 4.88, Classical); Leu249 (4.86, Classical); Asp285 (4.24, Classical; 4.94, Classical)	Ala248 (4.46, Alkyl); Leu249 (4.99, Alkyl)
HERP5 (Ctrl+)	Leu249 (3.92, Classical)	Ala248 (3.75, Pi/Alkyl; 7, Pi/Alkyl); Leu249 (4.59, Pi/Alkyl); Val250 (5.06, Pi/Alkyl); Tyr252 (5.05, Pi); Phe257 (5.25, Pi)

Ctrl+: positive-control

The effects of chrysin, chrysophanol, and chlorogenic acid on SKBR-3 (Figure 2a) and MCF-7 (Figure 2b) cell viability were determined by MTT assay. SKBR-3 and MCF-7 cells were treated with various concentrations of chrysin, chrysophanol, and chlorogenic acid (0, 100, 200, 400, 600, 800, and 1000 μ M) for 24, 48, and 72 h. As shown in Figure 2, they reduced the percentage of viable cells compared with untreated cells in a dose and time-dependent manner. However, the decrease in the percentage of viable SKBR-3 cells expressing high levels of HER-2 was more significant than that of MCF-7 cells. As shown in Table 5, chrysin's 50% inhibitory concentration (IC_{50}) value was less than other components. Based on the MTT assay outcomes, the concentrations of 200 μ M of chrysin and 600 μ M of both chrysophanol and chlorogenic acid were selected for further evaluation.

The scratch test was performed to detect the impact of chrysin, chrysophanol, and chlorogenic acid on the migration ability of SKBR-3 and MCF-7 cells. The results showed that they inhibited cell migration of the SKBR-3 cells, and the wound area remained unchanged, whereas the wound area percentage in the control group reduced in a time-dependent manner, particularly after 72 h (Figure 3a). Following the treatment of MCF-7 cells with chrysin, chrysophanol, and chlorogenic acid (Fig. 3b), the scratch gaps were observed to be filled with cells. Notably, chrysophanol treatment resulted in a more significant increase in cell migration at 48 and 72 h compared to chrysin and chlorogenic acid.

This data suggests that chrysin, chrysophanol, and chlorogenic acid could inhibit the migration of the cells specifically through inhibition of HER-2.

The effect of HER-2 inhibitor components on apoptosis was analyzed using the Annexin V/PI

assay. Flow cytometric analysis demonstrated that treatment of SKBR-3 with 200 μ M CH and 600 μ M CGA increased the percentage of total apoptotic cells up to 5.32% after 24 h and 19.1% after 48 h for chrysin (Figure 4b) and 1.27% after 24 h and 11.5% after 48h for chlorogenic acid (Figure 4c) compared to untreated cells (Figure 4a). Nevertheless, 200 μ M chrysin and 600 μ M chlorogenic acid did not induce apoptosis for MCF-7 cells as well as SKBR-3 cells. The total apoptotic rates for MCF-7 were 3.06 and 4.47 % after treatment with chrysin (Figure 4b), and 2.48 and 3.31 % after treatment with chlorogenic acid for 24 and 48 h, respectively (Figure 4c). Moreover, therapy with chrysophanol did not exhibit significant cell apoptosis in SKBR-3 and MCF-7 cell lines (data are not shown).

To discover the mechanisms involved in the apoptosis and migration of SKBR-3, the mRNA expression of caspase-3, CXCR4, and MMP9 were investigated in cells treated with 200 μ M of chrysin after 24 h. As shown in Figure 5, after treatment with chrysin, the mRNA expression levels of caspase-3 significantly increased in SKBR-3 ($p < 0.05$). In contrast, there was a marked decrease in mRNA expression of the CXCR4 gene in SKBR-3 cells in comparison with the control group ($p < 0.05$). The mRNA expression levels of VEGF and MMP9 genes were measured to evaluate the chrysin anti-angiogenic effect. Data analysis demonstrated that the chrysin did not affect MMP9 expression, while it could decrease the VEGF expression significantly in SKBR-3 cells ($p < 0.05$) but not in MCF-7.

In the current study, computational screening was employed to discover new potential herbal components for pharmaceutical research that effectively operate inhibitory activity on HER-2 for breast cancer. In this regard, 47 compounds in the PubChem database were used to select

desirable molecules and introduced as potential ligands using the AutoDock software. According to the docking analysis, three herbal components, chrysin, chrysophanol, and chlorogenic acid, demonstrated salient binding affinity to the HER-2 extracellular domain. The ΔG binding for these compounds was estimated to be -8.12 kcal/mol (for chrysin), -9.07 kcal/mol (for chrysophanol), and -10.20 kcal/mol (for chlorogenic acid). Based on the docking results, chlorogenic acid formed six hydrogens and two hydrophobic interactions with Ala248, Leu249, Asp285, and Val286 incorporated in the HER-2 extracellular domain. Chrysophanol showed three hydrogens

and four hydrophobic interactions with Cys293, Leu295, Asn297, Cys316, Ala317, and Val319 located in the HER-2 extracellular domain. Moreover, chrysin demonstrated five H-bond and three hydrophobic interactions with Cys246, Pro247, Ala248, Leu249, Val250, Tyr267, and Gly287. The molecular docking data showed considerable fitness with the MTT assay. However, the result did not completely coincide with the best compounds in the molecular mechanism of biological activities. Our data shows that chrysin significantly demonstrated the best anticancer activity in vitro for SKBR-3 cells compared to MCF-7.

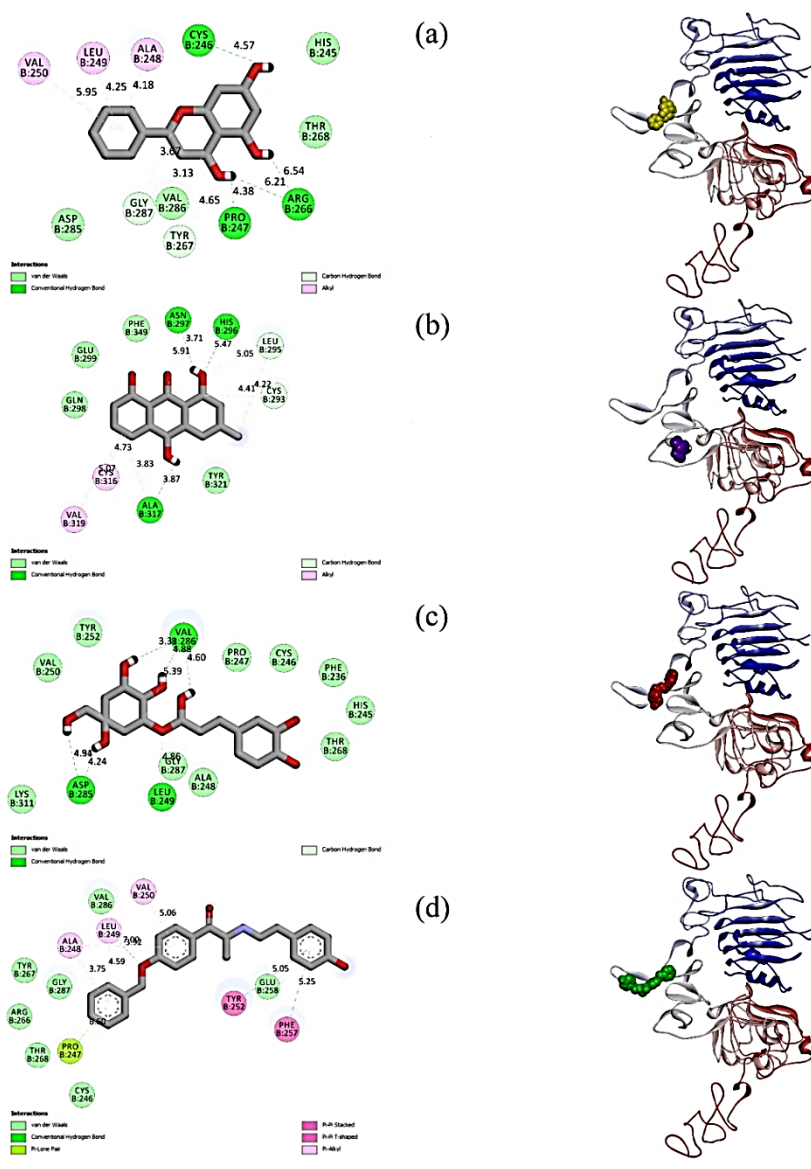


Figure 1. Two and three-dimensional views of the docked poses of chrysin (a), chrysophanol (b), chlorogenic acid (c), and the control inhibitor (d) within the HER-2 extracellular domain; all ligands are shown in CPK format in the three-dimensional images. HER-2: human epidermal growth factor receptor 2

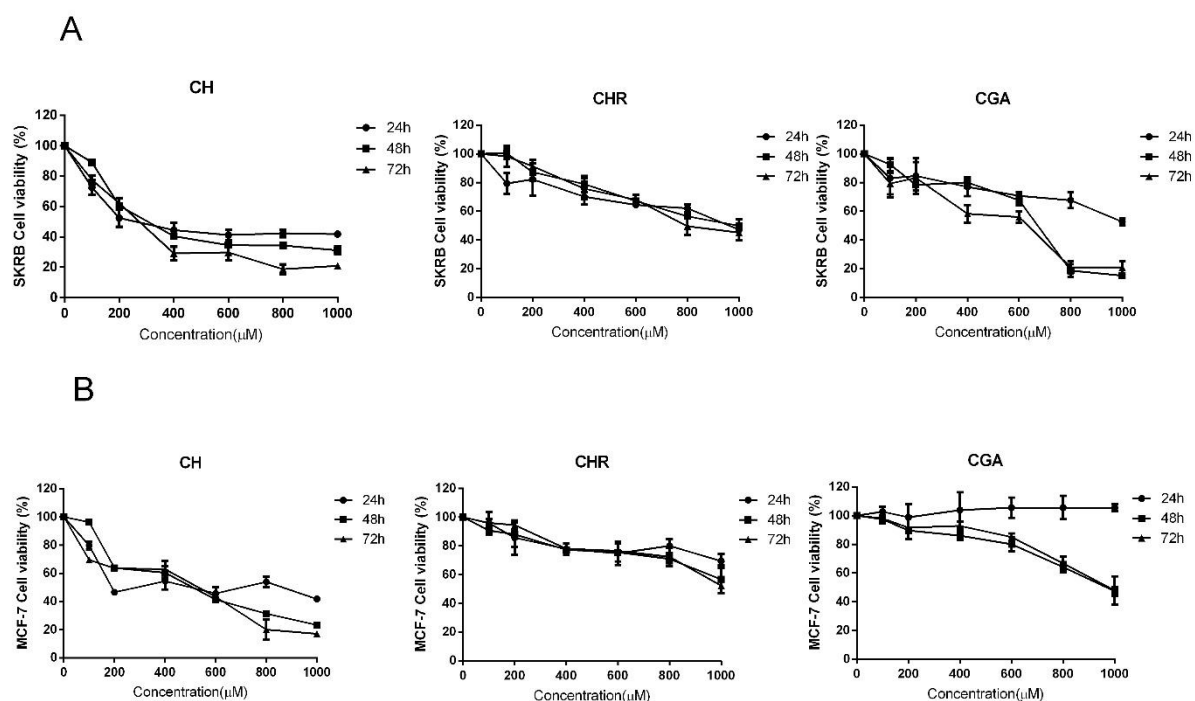


Figure 2. Effect of HER-2 inhibitors on cell viability; A) SKBR-3 and B) MCF-7 cells were treated with various concentrations of chrysin (CH), chrysoferanol (CHR), and chlorogenic acid (CGA) for 24, 48, and 72 h, and their viability was examined by MTT assay. Data are reported as the mean \pm standard error of the mean ($n = 8$)

Table 5. The IC_{50} values (μM) for chrysin, chrysoferanol, and chlorogenic acid

Compound	SKBR-3			MCF-7		
	24 h	48 h	72 h	24 h	48 h	72 h
CH	304.913	310.353	241.285	519.0269	427.686	513.71
CHR	877.764	980	883.363	4943.151	1848.59	1521.99
CGA	3091.98	361.434	319.256	Not significant	1024.17	1052.39

IC_{50} ; 50% inhibitory concentration; CH: chrysin; CHR: chrysoferanol; CGA: chlorogenic acid

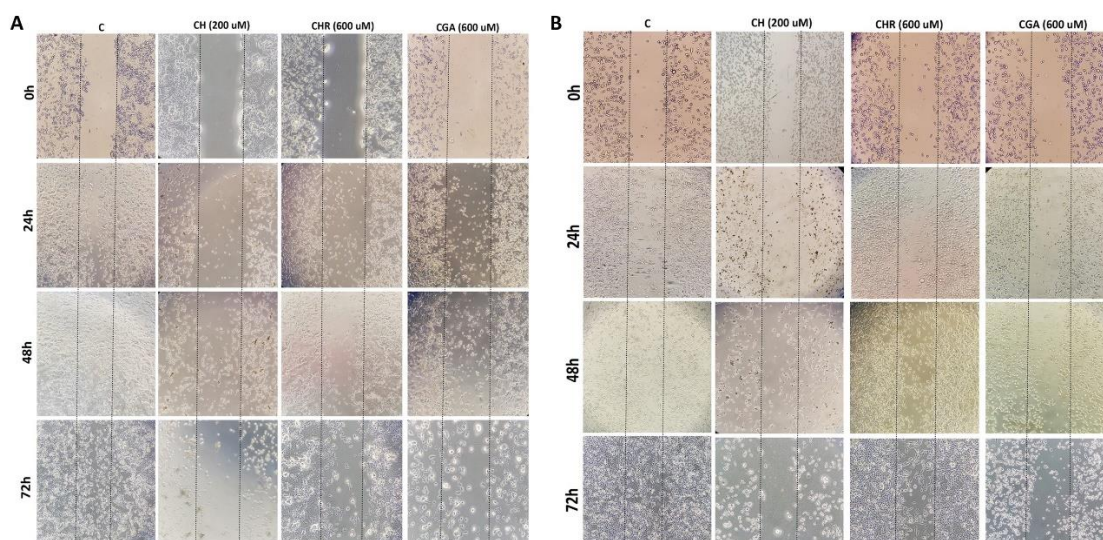


Figure 3. Effect of HER-2 inhibitors on cell migration; the migration capability of (a) SKBR-3 and (b) MCF-7 cells after 0, 24, 48, and 72 h of treatment with chrysin (CH), chrysoferanol (CHR), and chlorogenic acid (CGA)

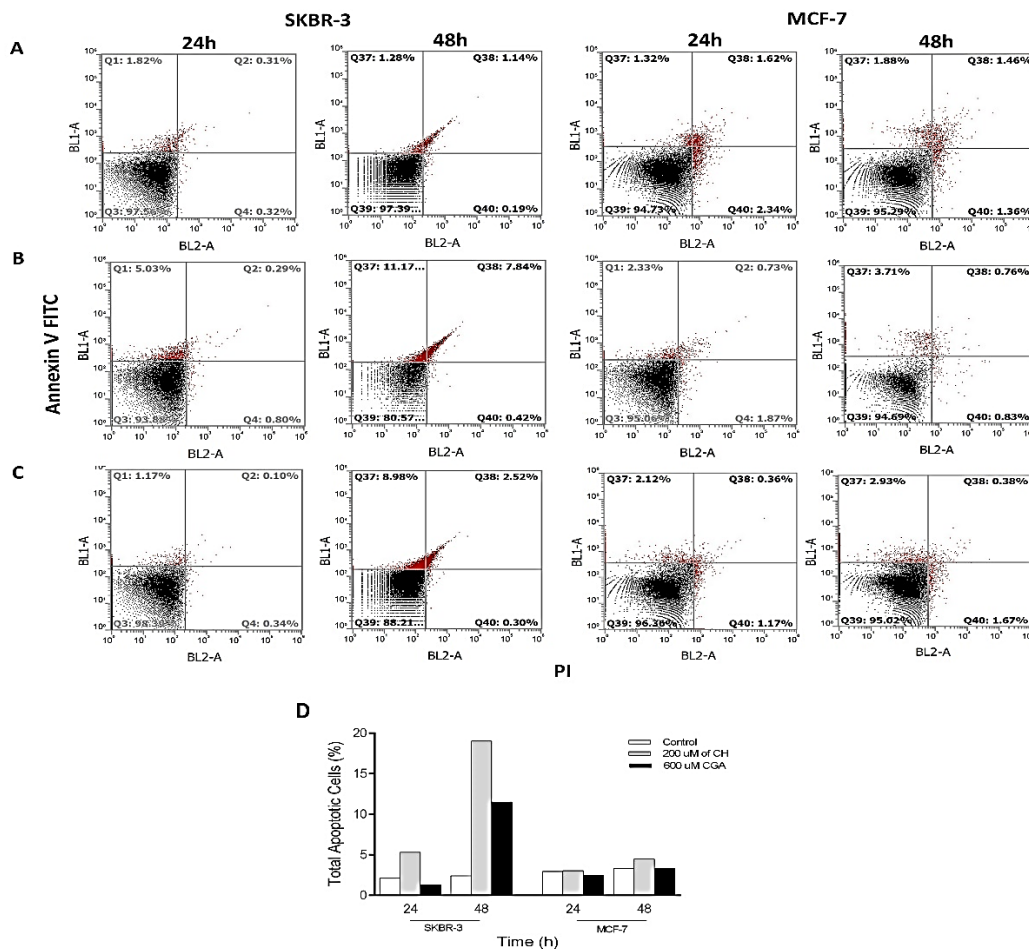


Figure 4. Effect of chrysin on apoptosis; representative flow cytometry plots of SKBR-3 and MCF-7 cells stained with propidium iodide/Annexin V-FITC at 24 and 48 h after treatment with A) 0 μM and B) 200 μM of chrysin (CH) C) 600 μM chlorogenic acid (CGA) (n=2); the total apoptotic rate of SKBR-3 cells was higher than MCF-7 cells; D) Percentage of total apoptotic cell after treatment

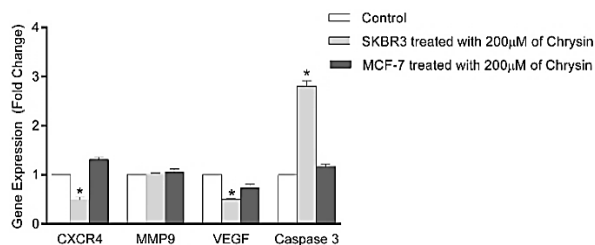


Figure 5. Effect of chrysin on cell migration, angiogenesis and apoptosis related genes; RT-qPCR analysis of CXCR4, MMP9, VEGF and caspase-3 expression in cells treated with chrysin and untreated cells after 24 h of treatment; data are represented as mean ± standard error of the mean (n = 3). *p<0.05 versus control group; qRT-PCR: quantitative reverse transcription PCR

Chrysin (5, 7-dihydroxyflavone) is a natural hydroxylated flavone that abundantly appears in some natural products, including honey, propolis, passion flowers, etc. Multiple pharmacological effects are displayed by chrysin, such as antibacterial, anticancer, anti-allergic, antihypertensive, anti-inflammatory, antidiabetic, anti-estrogenic, and antioxidant effects [1,83-86]. The antitumor cytotoxicity of chrysin has been widely studied over the years in many cancer types, such as hepatocellular, breast, prostate, and pancreatic carcinomas [87]. Moreover, to reduce the mechanisms of resistance in clinical cancer chemotherapy, chrysin was used with anticancer drugs such as doxorubicin, cisplatin, and ciglitazone to increase their cytotoxicity and induce apoptosis [88]. Regarding our results,

chrysin induced apoptosis of SKBR-3 cells through enhancement of caspase-3, but its effect on caspase-3 expression is not significant for MCF-7. A previous study confirmed that chrysin pretreatment diminished the viability of breast cancer cells through increased p53 protein expression for MCF-7 [89], up-regulation of S-phase kinase-associated protein-2 (Skp2), low-density lipoprotein receptor-related protein 6 (LRP6), peroxisome proliferator-activated receptor (PPAR α) and TRAIL-mediated apoptosis for MDA-MB-231 [90,91]. Chrysin showed a more accumulative inhibitory effect on the migration of SKBR-3 during 72 h compared to MCF-7. Chrysin also could reduce the migration and angiogenesis of SKBR-3 via downregulation of chemokine receptor CXCR4 and VEGF, respectively. In contrast, MMP9, as an intermediate molecule for migration and angiogenesis, was not affected by chrysin. As the same significant effects on the molecular mechanism were not seen for MCF-7, it can be considered that the inhibitory behavior of chrysin is related to the expression of HER-2. Lirdpramongkol et al. [92] reported that chrysin decreased the survival of 4T1 cells after exposure to hypoxia and suppressed hypoxia-induced VEGF gene expression. The combination treatment of apigenin and chrysin for 36 h synergistically decreased MDA-MB-231 cell motility through down-regulation of MMP2, MMP9, fibronectin, and snail [90]. In addition, chrysin demonstrated anticancer effects on SW620 cells by reducing the protein expression of p-ERK/ERK, p-AKT/AKT, amphiregulin, CXCL1, and MMP-9 were identified as potential targets for chrysin [93].

Chlorogenic acid, a well-known polyphenol, is an ester formed from cinnamic acids and quinic acid produced by certain plant species and is an essential component of green coffee beans. Evidence has established that this substance possesses different biological properties, including antioxidant and anticarcinogenic activities and antibacterial, particularly antidiabetic and antilipidemic effects [94]. In a study by Park et al., chlorogenic acid could inhibit hypoxia-induced angiogenesis in HUVEC cells by downregulating the HIF-1 α /AKT pathway [95]. Chlorogenic acid also induces the differentiation of solid tumor cells through the expression of KHSRP, p53, and p21 and attenuates the cancer behavior leading to being

considered a promising therapeutic agent for cancer [96]. Additionally, Zeng et al. demonstrated that chlorogenic acid could significantly suppress viability and induce apoptosis in breast cancer cells. Chlorogenic acid suppressed the migration and invasion of breast cancer cells by impairing the NF- κ B/EMT signaling pathway and improved antitumor immunity by enhancing the proportion of CD4⁺ and CD8⁺ T cells in the spleens of mice-bearing tumors [97]. Our data also confirmed that chlorogenic acid could decline breast cancer cells' viability and migration ability.

Chrysophanol is a naturally occurring anthraquinone that was initially extracted from plants of the *Rheum* genus. In parallel with our results, it has been demonstrated that chrysophanol has anticancer properties. It induces cell death of human liver cancer cells by stimulating intracellular production of reactive oxygen species (ROS) production and impairing mitochondrial ATP synthesis [98]. Also, chrysophanol preferentially inhibits the viability of colon cancer cells, which express a high level of EGFR via suppression of EGF-induced phosphorylation of EGFR and downstream signaling molecules, such as AKT, ERK, and mTOR [99]. In the study by Wang et al. chrysophanol inhibited the growth of meningioma cells by modulating osteoglycin/mTOR and NF2 signaling pathways. Chrysophanol treatment significantly diminished the Bcl-2/Bax expression ratio, up-regulated cleaved caspase-3 and -9, and the activities of caspase-3 and -9 [100]. Moreover, chrysophanol effectively suppressed breast cancer cell proliferation and facilitated chemosensitivity to paclitaxel through modulation of NF- κ B/cyclin signaling [101]. These data align with our results, which showed the inhibitory effect of chrysophanol on breast cancer cells survival and migration, especially on SKBR-3.

In future studies, more analyses (e.g., cell apoptosis assay, AOPI staining, cell cycle analysis, and western blot test) should be performed to confirm our findings and to illustrate more molecular mechanisms of chrysin.

Conclusion

The present study provided accurate preliminary information for recognizing novel natural HER-2 inhibitors using in silico pharmacophore-based screening. The molecular docking identified three

compounds as possible HER-2 inhibitors with drug-like features based on optimal binding modes, binding affinities, and critical interactions. Their inhibitory biological activity also demonstrated that chrysin, chrysophanol, and chlorogenic acid could selectively inhibit the proliferation and migration of HER-2-positive breast cancer cells. The natural compound chrysin was identified as a potential inhibitor against HER-2 based on in silico and experimental analysis. This study could suggest a way to develop selective and safer HER-2 inhibitors with a superior therapeutic profile in future studies.

Acknowledgments

The authors would like to thank the Deputy of Research and Technology, and Research Center for Molecular Medicine, Hamadan University of Medical Sciences, Hamadan, Iran for their supports. This study was funded by the Research Center for Molecular Medicine, Hamadan University of Medical Sciences, Hamadan, Iran (Research ID: 9812069415).

Author contributions

Amir Taherkhani, Massoud Saidijam, Naghmeh Shirafkan, and Mona Pourjafar, designed the study. The in silico analysis were conducted and interpreted by Amir Taherkhani and Somaye Bakhtiari. In vitro experiments were executed by Mona Pourjafar and Naghmeh Shirafkan. The results were analyzed and discussed by Mona Pourjafar, Amir Taherkhani, Naghmeh Shirafkan, Somaye Bakhtiari, Saeid Afshar, and Alireza Jalalvand. Mona Pourjafar and Amir Taherkhani wrote the manuscript. Naghmeh Shirafkan, Saeid Afshar, and Alireza Jalalvand edited the manuscript. All authors read and approved the final version of the manuscript.

Declaration of interest

The authors declare that there is no conflict of interest. The authors alone are responsible for the accuracy and integrity of the paper content.

References

[1] Gresa-Arribas N, Serratos J, Saura J, Solà C. Inhibition of CCAAT/enhancer binding protein δ expression by chrysin in microglial cells results in anti-inflammatory and neuroprotective effects. *J Neurochem.* 2010; 115(2): 526–536.

- [2] Harborg S, Zachariae R, Olsen J, Johannsen M, Cronin-Fenton D, Boggild H, Borgquist S. Overweight and prognosis in triple-negative breast cancer patients: a systematic review and meta-analysis. *NPJ Breast Cancer.* 2021; 7(1): 1–9.
- [3] Johnson KS, Conant EF, Soo M. Molecular subtypes of breast cancer: a review for breast radiologists. *J Breast Imaging.* 2021; 3(1): 12–24.
- [4] Malhotra GK, Zhao X, Band H, Band VJCB. Histological, molecular and functional subtypes of breast cancers. *Cancer Biol Ther.* 2010; 10(10): 955–960.
- [5] Samadi P, Saki S, Dermani FK, Pourjafar M, Saidijam MJCO. Emerging ways to treat breast cancer: will promises be met? *Cell Oncol.* 2018; 41(6): 605–621.
- [6] Loibl S, Gianni LJTL. HER2-positive breast cancer. *Lancet.* 2017; 389(10087): 2415–2429.
- [7] Arteaga CL, Sliwkowski MX, Osborne CK, Perez EA, Puglisi F, Gianni L. Treatment of HER2-positive breast cancer: current status and future perspectives. *Nat Rev Clin Oncol.* 2012; 9(1): 16–32.
- [8] Wang J, Xu B. Targeted therapeutic options and future perspectives for HER2-positive breast cancer. *Signal Transduct Target Ther.* 2019; 4(1): 1–22.
- [9] Li J, Wang H, Li J, Bao J, Wu C. Discovery of a potential HER2 inhibitor from natural products for the treatment of HER2-positive breast cancer. *Int J Mol Sci.* 2016; 17(7): 1–14.
- [10] Tasleem M, Alrehaily A, Almeleebia TM, Alshahrani MY, Ahmad I, Asiri M, Alabdallah NM, Saeed M. Investigation of antidepressant properties of yohimbine by employing structure-based computational assessments. *Curr Issues Mol Biol.* 2021; 43(3): 1805–1827.
- [11] Tavakoli J, Miar S, Zadehzare MM, Akbari H. Evaluation of effectiveness of herbal medication in cancer care: a review study. *Iran J Cancer Prev.* 2012; 5(3): 144–156.
- [12] Taherkhani A, Moradkhani S, Orangi A, Jalalvand A, Khamverdi Z. Molecular docking study of flavonoid compounds for possible matrix metalloproteinase-13 inhibition. *J Basic Clin Physiol Pharmacol.* 2021; 32(6): 1105–1119.
- [13] Taherkhani A, Orangi A, Moradkhani S,

- Khamverdi Z. Molecular docking analysis of flavonoid compounds with matrix metalloproteinase-8 for the identification of potential effective inhibitors. *Lett Drug Des Discov*. 2021; 18(1): 16–45.
- [14] Taherkhani A, Moradkhani S, Orangi A, Jalalvand A. In silico study of some natural anthraquinones on matrix metalloproteinase inhibition. *Res J Pharmacogn*. 2021; 8(4): 37–51.
- [15] Taherkhani A, Orangi A, Moradkhani S, Jalalvand A, Khamverdi Z. Identification of potential anti-tooth-decay compounds from organic cinnamic acid derivatives by inhibiting matrix metalloproteinase-8: an in silico study. *Avicenna J Dent Res*. 2022; 14(1): 25–32.
- [16] Taherkhani A, Ghonji F, Mazaheri A, Lohrasbi MP, Mohamadi Z, Khamverdi Z. Identification of potential glucosyltransferase inhibitors from cinnamic acid derivatives using molecular docking analysis: a bioinformatics study. *Avicenna J Clin Microbiol Infect*. 2021; 8(4): 145–155.
- [17] Kopustinskiene DM, Jakstas V, Savickas A, Bernatoniene J. Flavonoids as anticancer agents. *Nutrients*. 2020; 12(2): 1–25.
- [18] Malik MS, Alsantali RI, Jassas RS, Alsimaree AA, Syed R, Alsharif MA, Kalpana K, Morad M, Althagafi II, Ahmed SA. Journey of anthraquinones as anticancer agents - a systematic review of recent literature. *RCS Adv*. 2021; 11(57): 35806–35827.
- [19] De P, Baltas M, Bedos-Belval F. Cinnamic acid derivatives as anticancer agents-a review. *Curr Med Chem*. 2011; 18(11): 1672–1703.
- [20] Pontiki E, Hadjipavlou-Litina D, Litinas K, Geromichalos G. Novel cinnamic acid derivatives as antioxidant and anticancer agents: design, synthesis and modeling studies. *Molecules*. 2014; 19(7): 9655–9674.
- [21] Saeed M, Tasleem M, Shoib A, Kausar MA, Sulieman AME, Alabdallah NM, Asmar Z, Abdelgadir A, Al-Shamari A, Alam MJ. Identification of putative plant-based ALR-2 inhibitors to treat diabetic peripheral neuropathy. *Curr Issues Mol Biol*. 2022; 44(7): 2825–2841.
- [22] Franklin MC, Carey KD, Vajdos FF, Leahy DJ, de Vos AM, Sliwkowski MX. Insights into ErbB signaling from the structure of the ErbB2-pertuzumab complex. *Cancer Cell*. 2004; 5(4): 317–328.
- [23] Rose PW, Prlić A, Altunkaya A, Bi C, Bradley AR, Christie CH, Costanzo LD, Duarte JM, Dutte S, Feng Z. The RCSB protein data bank: integrative view of protein, gene and 3D structural information. *Nucleic Acids Res*. 2016; 45(1): 271–281.
- [24] Satyanarayanajois S, Villalba S, Jianchao L, Lin GM. Design, synthesis, and docking studies of peptidomimetics based on HER2–herceptin binding site with potential antiproliferative activity against breast cancer cell lines. *Chem Biol Drug Des*. 2009; 74(3): 246–257.
- [25] Guex N, Peitsch MC, Schwede T. Automated comparative protein structure modeling with SWISS-MODEL and Swiss-PdbViewer: a historical perspective. *Electrophoresis*. 2009; 30(S1): 162–173.
- [26] Tasleem M, Ishrat R, Islam A, Ahmad F, Hassan I. Structural characterization, homology modeling and docking studies of ARG674 mutation in MyH8 gene associated with trismus-pseudocamptodactyly syndrome. *Lett Drug Des Discov*. 2014; 11(10): 1177–1187.
- [27] Laxmi D, Priyadarshy S. HyperChem 6.03. *Biotech Softw Internet Rep*. 2002; 3(1): 5–9.
- [28] Morris GM, Huey R, Olson AJ. Using autodock for ligand-receptor docking. *Curr Protoc Bioinform*. 2008; 24(1): 8–14.
- [29] Bamehr H, Saidijam M, Dastan D, Amini R, Pourjafar M, Najafi R. *Ferula pseudalliacea* induces apoptosis in human colorectal cancer HCT-116 cells via mitochondria-dependent pathway. *Arch Physiol Biochem*. 2019; 125(3): 284–291.
- [30] Rezaeepoor M, Rashidi G, Pourjafar M, Mohammadi C, Solgi G, Najafi R. SEMA4D Knockdown attenuates β -catenin-dependent tumor progression in colorectal cancer. *Biomed Res Int*. 2021; Article ID 8507373.
- [31] Gaillard T. Evaluation of autodock and autodock vina on the CASF-2013 benchmark. *J Chem Inf Model*. 2018; 58(8): 1697–1706.
- [32] Naz S, Imran M, Rauf A, Orhan IE, Shariati MA, Shahbaz M, Qaisrani TB, Shah ZA, Plygun S, Heydari M. Chrysin: pharmacological and therapeutic properties. *Life Sci*. 2019; 235: 1–10.
- [33] Chin YW, Jung HA, Liu Y, Su BN, Castoro JA, Keller WJ, Pereira MA, Kinghorn AD. Antioxidant constituents of the roots and

- stolons of licorice (*Glycyrrhiza glabra*). *J Agric Food Chem*. 2007; 55(12): 4691–4697.
- [34] Salehi B, Venditti A. The therapeutic potential of apigenin. *Int J Mol Sci*. 2019; 20(6): 1–26.
- [35] Guo Y, Li D, Cen XF, Qiu HL, Ma YL, Liu Y, Huang SH, Liu LB, Xu M, Tang QZ. Diosmetin protects against cardiac hypertrophy via p62/Keap1/Nrf2 signaling pathway. *Oxid Med Cell Longev*. 2022; Article ID 8367997.
- [36] Peng L, Gao X, Nie L, Xie J, Dai T, Shi C, Tao L, Wang Y, Tian Y, Sheng J. Astragalin attenuates dextran sulfate sodium (DSS)-induced acute experimental colitis by alleviating gut microbiota dysbiosis and inhibiting NF- κ B activation in Mice. *Front Immunol*. 2020; 11: 1–13.
- [37] Gilani SJ, Bin-Jumah MN, Al-Abbasi FA, Nadeem MS, Imam SS. Protective effect of fustin against ethanol-activated gastric ulcer via downregulation of biochemical parameters in rats. *ACS Omega*. 2022; 7(27): 23245–23254.
- [38] Hong A. Antimicrobial activities of tea-derived flavonoids against skin staphylococci. Undergraduate thesis. Department of Math-Science, College of Arts & Sciences, Concordia University, Portland. U.S, 2017.
- [39] Stevens JF, Taylor AW, Nickerson GB, Ivancic M, Henning J, Haunold A, Deinzer ML. Prenylflavonoid variation in *Humulus lupulus*: distribution and taxonomic significance of xanthogalenol and 4'-O-methylxanthohumol. *Phytochemistry*. 2000; 53(7): 759–775.
- [40] Peng F, Du Q, Peng C, Wang N, Tang H, Xie X, Shen J, Chen J. A review: the pharmacology of isoliquiritigenin. *Phytother Res*. 2015; 29(7): 969–977.
- [41] Thong NM, Vo QV, Huyen TL, Bay MV, Tuan D, Nam PC. Theoretical study for exploring the diglycoside substituent effect on the antioxidative capability of isorhamnetin extracted from *anoectochilus roxburghii*. *ACS Omega*. 2019; 4(12): 14996–15003.
- [42] Gong Y, Fang F, Zhang X, Liu B, Luo H, Li Z, Zhang X, Zhang Z, Pang X. B type and complex A/B type epicatechin trimers isolated from litchi pericarp aqueous extract show high antioxidant and anticancer activity. *Int J Mol Sci*. 2018; 19(1): 1–19.
- [43] Wang MC, Huang WC. Sophoraflavanone G from *Sophora flavescens* ameliorates allergic airway inflammation by suppressing Th2 response and oxidative stress in a murine asthma model. *Int J Mol Sci*. 2022; 23(11): 1–15.
- [44] Hu S, Wang D, Wang W, Zhang C, Li Y, Wang Y, Zhou W, Niu J, Wang S, Qiang Y. Whole genome and transcriptome reveal flavone accumulation in *Scutellaria baicalensis* roots. *Front Plant Sci*. 2022; 13: 1–13.
- [45] Karancsi Z, Kovács D. The impact of quercetin and its methylated derivatives 3-O-methylquercetin and rhamnazin in lipopolysaccharide-induced inflammation in porcine intestinal cells. *Antioxidants*. 2022; 11(7): 1–12.
- [46] Kang GD, Kim DH. Ponciretin attenuates ethanol-induced gastric damage in mice by inhibiting inflammatory responses. *Int immunopharmacol*. 2017; 43: 179–186.
- [47] Simmler C, Pauli GF, Chen SN. Phytochemistry and biological properties of glabridin. *Fitoterapia*. 2013; 90: 160–184.
- [48] Muhammad T, Ikram M, Ullah R, Rehman SU, Kim MO. Hesperetin, a citrus flavonoid, attenuates LPS-induced neuroinflammation, apoptosis and memory impairments by modulating TLR4/NF- κ B signaling. *Nutrients*. 2019; 11(3): 1–20.
- [49] Reddy UDC, Chawla AS, Deepak M, Singh D, Handa SS. High pressure liquid chromatographic determination of bergenin and (+)-afzelechin from different parts of Paashaanbhed (*Bergenia ligulata* Yeo). *Phytochem Anal*. 1999; 10(1): 44–47.
- [50] Egler J, Lang F. Licochalcone a induced suicidal death of human erythrocytes. *Cell Physiol Biochem*. 2015; 37(5): 2060–2070.
- [51] Aydin T, Bayrak N, Baran E, Cakir A. Insecticidal effects of extracts of *Humulus lupulus* (hops) L. cones and its principal component, xanthohumol. *Bull Entomol Res*. 2017; 107(4): 543–549.
- [52] Lima Cavendish R, de Souza Santos J, Belo Neto R, Oliveira Paixao A, Valeria Oliveira J, Divino de Araujo ED, Silva AA, Thomazzi SM, Cardoso JC, Gomes MZ. Antinociceptive and anti-inflammatory effects of Brazilian red propolis extract and formononetin in rodents. *J Ethnopharmacol*. 2015; 173: 127–133.

- [53] Yusuf MA, Singh BN, Sudheer S, Kharwar RN, Siddiqui S, Abdel-Azeem AM, Fernandes L, Dashora K, Gupta VK. Chrysophanol: a natural anthraquinone with multifaceted biotherapeutic potential. *Biomolecules*. 2019; 9(2): 1–24.
- [54] Xu Z, Hou Y, Zou C, Liang H, Mu J, Jiao X, Zhu Y, Su L, Liu M, Chen X. Alizarin, a nature compound, inhibits the growth of pancreatic cancer cells by abrogating NF- κ B activation. *Int J Biol Sci*. 2022; 18(7): 2759–2774.
- [55] Nair DA, James T, Sreelatha S, Kariyil BJ. Antioxidant and antiproliferative properties of *Moringa oleifera* Lam. leaf aqueous extract. *Plant Sci Today*. 2020; 7(4): 649–657.
- [56] Zhou YX, Xia W, Yue W, Peng C, Rahman K, Zhang H. Rhein: a review of pharmacological activities. *Evid Based Complement Altern Med*. 2015; Article ID 578107.
- [57] Krivoshchekova O, Maximov O, Stepanenko L, Mishchenko N. Quinones of the lichen *Cetraria cucullata*. *Phytochemistry*. 1982; 21(1): 193–196.
- [58] Dong X, Fu J, Yin X, Cao S, Li X, Lin L, Huyiligeqi, Ni J. Emodin: a review of its pharmacology, toxicity and pharmacokinetics. *Phytother Res*. 2016; 30(8): 1207–1218.
- [59] Tseng CC, Lai YC, Kuo TJ, Su JH, Sung PJ. Rhodoptilometrin, a crinoid-derived anthraquinone, induces cell regeneration by promoting wound healing and oxidative phosphorylation in human gingival fibroblast cells. *Mar Drugs*. 2019; 17(3): 1–20.
- [60] Dong X, Wang L, Song G, Cai X, Wang W, Chen J, Wang G. Physcion protects rats against cerebral ischemia-reperfusion injury via inhibition of TLR4/NF- κ B signaling pathway. *Drug Des Devel Ther*. 2021; 15: 277–287.
- [61] Akao T, Che QM, Kobashi K, Yang L, Hattori M, Namba T. Isolation of a human intestinal anaerobe, *Bifidobacterium* sp. strain SEN, capable of hydrolyzing sennosides to sennidins. *Appl Environ Microbiol*. 1994; 60(3): 1041–1043.
- [62] Shi X, Zhang Y, Lin B, Zhou Y, Suo W, Wei J, Zhang L, Lin J, Xiao F, Zhao L. Danthron attenuates experimental atherosclerosis by targeting foam cell formation. *Exp Physiol*. 2021; 106(3): 653–662.
- [63] Chitsaz R, Zarezadeh A, Asgarpanah J. Rubiadin exerts an acute and chronic anti-inflammatory effect in rodents. *Braz J Biol*. 2021; 83: 1–8.
- [64] Park EJ, Park K. Potent and selective inhibition of CYP1A2 enzyme by obtusifolin and its chemopreventive effects. *Pharmaceutics*. 2022; 14(12): 1–14.
- [65] Ji Y, Jiang C, Zhang X, Liu W, Gao M, Li Y, Wang J, Wang Q, Sun Z, Jiang X. Necrosis targeted combinational theragnostic approach using radioiodinated sennidin A in rodent tumor models. *Oncotarget*. 2014; 5(10): 2934–2946.
- [66] Woradulayapinij W, Pothiluk A, Nuansanit T, Yimsoo T, Yingmema W, Rojanapanthu P, Hong Y, Baek SJ, Treesuppharat W. Acute oral toxicity of damnacanthal and its anticancer activity against colorectal tumorigenesis. *Toxicol Rep*. 2022; 9: 1968–1976.
- [67] Wube AA, Bucar F, Asres K, Gibbons S, Adams M, Streit B, Bodensieck A, Bauer R. Knipholone, a selective inhibitor of leukotriene metabolism. *Phytomedicine*. 2006; 13(6): 452–456.
- [68] Latifah SY, Gopalsamy B, Abdul Rahim R, Manaf Ali A, Haji Lajis N. Anticancer potential of damnacanthal and nordamnacanthal from morinda elliptica roots on T-lymphoblastic leukemia cells. *Molecules*. 2021; 26(6): 1–20.
- [69] Santana-Gálvez J, Cisneros-Zevallos L, Jacobo-Velázquez DA. Chlorogenic acid: recent advances on its dual role as a food additive and a nutraceutical against metabolic syndrome. *Molecules*. 2017; 22(3): 1–21.
- [70] Da Cunha FM, Duma D, Assreuy J, Buzzi FC, Niero R, Campos MM, Calixto JB. Caffeic acid derivatives: in vitro and in vivo anti-inflammatory properties. *Free Radic Res*. 2004; 38(11): 1241–1253.
- [71] Dai G, Jiang Z, Sun B, Liu C, Meng Q, Ding K, Jing W, Ju W. Caffeic acid phenethyl ester prevents colitis-associated cancer by inhibiting NLRP3 inflammasome. *Front Oncol*. 2020; 10: 1–12.
- [72] Shahidi F, Chandrasekara A. Hydroxycinnamates and their in vitro and in vivo antioxidant activities. *Phytochem Rev*. 2010; 9(1): 147–170.
- [73] Budryn G, Nebesny E. Phenolic acids - their properties, occurrence, in plant raw materials,

- absorption, and metabolic transformations. *Bromatol Chem.* 2006; 39(2): 103–110.
- [74] Salameh D, Brandam C, Medawar W, Lteif R, Strehaiano P. Highlight on the problems generated by p-coumaric acid analysis in wine fermentations. *Food Chem.* 2008; 107(4): 1661–1667.
- [75] Kowczyk-Sadowy M, Świsłocka R, Lewandowska H, Piekut J, Lewandowski W. Spectroscopic (FT-IR, FT-Raman, 1H- and 13C-NMR), theoretical and microbiological study of trans o-coumaric acid and alkali metal o-coumarates. *Molecules.* 2015; 20(2): 3146–3169.
- [76] United States Department of Agriculture. Dr. Duke's Phytochemical and ethnobotanical databases. [Accessed 2023]. Available from: <https://phytochem.nal.usda.gov/>.
- [77] Masi M, Koirala M, Delicato A. Isolation and biological characterization of homoisoflavanoids and the alkylamide N-p-coumaroyltyramine from *Crinum biflorum* Rottb., an amaryllidaceae species collected in Senegal. *Biomolecules.* 2021; 11(9): 1–21.
- [78] Silva H, Lopes NMF. Cardiovascular effects of caffeic acid and its derivatives: a comprehensive review. *Front Physiol.* 2020; 11: 1–20.
- [79] Ruwizhi N, Aderibigbe BA. Cinnamic acid derivatives and their biological efficacy. *Int J Mol Sci.* 2020; 21(16): 1–34.
- [80] Zduńska K, Dana A, Kolodziejczak A, Rotsztejn H. Antioxidant properties of ferulic acid and its possible application. *Skin Pharmacol Physiol.* 2018; 31(6): 332–336.
- [81] Senawong T, Misuna S, Khaopha S, Nuchadomrong S, Sawatsitang P, Phaosiri C, Surapaitoon A, Sripan B. Histone deacetylase (HDAC) inhibitory and antiproliferative activities of phenolic-rich extracts derived from the rhizome of *Hydnophytum formicarum* Jack.: sinapinic acid acts as HDAC inhibitor. *BMC Complement Altern Med.* 2013; 13: 1–11.
- [82] Triptow J, Meijer G, Fielicke A, Dopfer O, Green M. Comparison of conventional and nonconventional hydrogen bond donors in Au-complexes. *J Phys Chem.* 2022; 126(24): 3880–3892.
- [83] Parajuli P, Joshee N, Rimando AM, Mittal S, Yadav AK. In vitro antitumor mechanisms of various *Scutellaria* extracts and constituent flavonoids. *Planta Med.* 2009; 75(1): 41–48.
- [84] Torres-Piedra M, Ortiz-Andrade R, Villalobos-Molina R, Singh N, Medina-Franco JL, Webster SP, Binnie M, Navarrete G, Estrada-Soto S. A comparative study of flavonoid analogues on streptozotocin–nicotinamide induced diabetic rats: quercetin as a potential antidiabetic agent acting via 11 β -hydroxysteroid dehydrogenase type 1 inhibition. *Eur J Med Chem.* 2010; 45(6): 2606–2612.
- [85] Wang J, Qiu J, Dong J, Li H, Luo M, Dai X, Zhang Y, Leng B, Niu X, Zhao S. Chrysin protects mice from *Staphylococcus aureus* pneumonia. *J Appl Microbiol.* 2011; 111(6): 1551–1558.
- [86] Xu Y, Tong Y, Ying J, Lei Z, Wan L, Zhu X, Ye F, Mao P, Wu X, Pan R. Chrysin induces cell growth arrest, apoptosis, and ER stress and inhibits the activation of STAT3 through the generation of ROS in bladder cancer cells. *Oncol Lett.* 2018; 15(6): 9117–9125.
- [87] Liu D, Li YP, Shen HX, Li Y, He J, Zhang QZ, Liu YM. Synthesis and antitumor activities of novel 7-O-amino acids chrysin derivatives. *Chin Herb Med.* 2018; 10(3): 323–330.
- [88] Kasala ER, Bodduluru LN, Madana RM, Gogoi R, Barua CCJTL. Chemopreventive and therapeutic potential of chrysin in cancer: mechanistic perspectives. *Toxicol Lett.* 2015; 233(2): 214–225.
- [89] Nagasaka M, Hashimoto R, Inoue Y, Ishiuchi Ki, Matsuno M, Itoh Y, Tokugawa M, Ohoka N, Morishita D, Mizukami H. Anti-tumorigenic activity of chrysin from *Oroxylum indicum* via non-genotoxic p53 activation through the ATM-Chk2 pathway. *Molecules.* 2018; 23(6): 1–13.
- [90] Huang C, Wei YX, Shen MC, Tu YH, Wang CC, Huang HC. Chrysin, abundant in *Morinda citrifolia* fruit water–etoac extracts, combined with apigenin synergistically induced apoptosis and inhibited migration in human breast and liver cancer cells. *J Agric Food Chem.* 2016; 64(21): 4235–4245.
- [91] Hong TB, Rahumatullah A, Yogarajah T, Ahmad M, Yin KB. Potential effects of chrysin on MDA-MB-231 cells. *Int J Mol Sci.* 2010; 11(3): 1057–1069.
- [92] Lirdprapamongkol K, Sakurai H, Abdelhamed S, Yokoyama S, Maruyama T, Athikomkulchai S, Viriyaroj A, Awale S, Yagita H, Ruchirawat S. A flavonoid chrysin

- suppresses hypoxic survival and metastatic growth of mouse breast cancer cells. *Oncol Rep.* 2013; 30(5): 2357–2364.
- [93] Salama AA, Allam RM. Promising targets of chrysin and daidzein in colorectal cancer: Amphiregulin, CXCL1, and MMP-9. *Eur J Pharmacol.* 2021; Article ID 173763.
- [94] Yang YQ, Yan C, Branford-White CJ, Hou XY. Biological values of acupuncture and Chinese herbal medicine: impact on the life science. *Evid Based Complement Altern Med.* 2014; Article ID 593921.
- [95] Park JJ, Hwang SJ, Park JH, Lee HJ. Chlorogenic acid inhibits hypoxia-induced angiogenesis via down-regulation of the HIF-1 α /AKT pathway. *Cell Oncol.* 2015; 38(2): 111–118.
- [96] Huang S, Wang LL, Xue NN, Li C, Guo HH, Ren TK, Zhan Y, Li WB, Zhang J, Chen XG. Chlorogenic acid effectively treats cancers through induction of cancer cell differentiation. *Theranostics.* 2019; 9(23): 6745–6763.
- [97] Zeng A, Liang X, Zhu S, Liu C, Wang S, Zhang Q, Zhao J, Song L. Chlorogenic acid induces apoptosis, inhibits metastasis and improves antitumor immunity in breast cancer via the NF- κ B signaling pathway. *Oncol Rep.* 2021; 45(2): 717–727.
- [98] Lu CC, Yang JS, Huang AC, Hsia TC, Chou ST, Kuo CL, Lu HF, Lee TH, Wood WG, Chung JG. Chrysophanol induces necrosis through the production of ROS and alteration of ATP levels in J5 human liver cancer cells. *Mol Nutr Food Res.* 2010; 54(7): 967–976.
- [99] Lee MS, Cha EY, Sul JY, Song IS, Kim JYJPR. Chrysophanic acid blocks proliferation of colon cancer cells by inhibiting EGFR/mTOR pathway. *Phytother Res.* 2011; 25(6): 833–837.
- [100] Wang J, Lv PJB. Chrysophanol inhibits the osteoglycin/mTOR and activates NF2 signaling pathways to reduce viability and proliferation of malignant meningioma cells. *Bioengineered.* 2021; 12(1): 755–762.
- [101] Ren L, Li Z, Dai C, Zhao D, Wang Y, Ma C, Liu C. Chrysophanol inhibits proliferation and induces apoptosis through NF- κ B/cyclin D1 and NF- κ B/Bcl-2 signaling cascade in breast cancer cell lines. *Mol Med Rep.* 2018; 17(3): 4376–4382.

Abbreviations

CH: chrysin; CHR: chrysophanol; CGA: chlorogenic acid; HER-2: human epidermal growth factor receptor 2; IC₅₀: 50% inhibitory concentration